Electron Supplementary Information for:

Facile Synthesis and Surface Modification of Bioinspired Nanoparticles from Quercetin for Drug Delivery

Suhair Sunoqrot[a,b]*, Eveen Al-Shalabi[a], and Phillip B. Messersmith[b,c,d]

[a]Department of Pharmacy, Faculty of Pharmacy, Al-Zaytoonah University of Jordan, Amman 11733, Jordan
Departments of [b]Bioengineering and [c]Materials Science and Engineering, University of California, Berkeley, CA 94720, USA
[d]Materials Sciences Division, Lawrence Berkeley National Laboratory, Berkeley, CA 94720, USA

***Corresponding Author:**
Suhair Sunoqrot, PhD
Assistant Professor of Pharmaceutics
Department of Pharmacy
Faculty of Pharmacy
Al-Zaytoonah University of Jordan
P.O. Box 130, Amman 11733, Jordan
Phone: +962-6-4291511 Ext. 312
Fax: +962-6-4291432
Email: suhair.sunoqrot@zuj.edu.jo

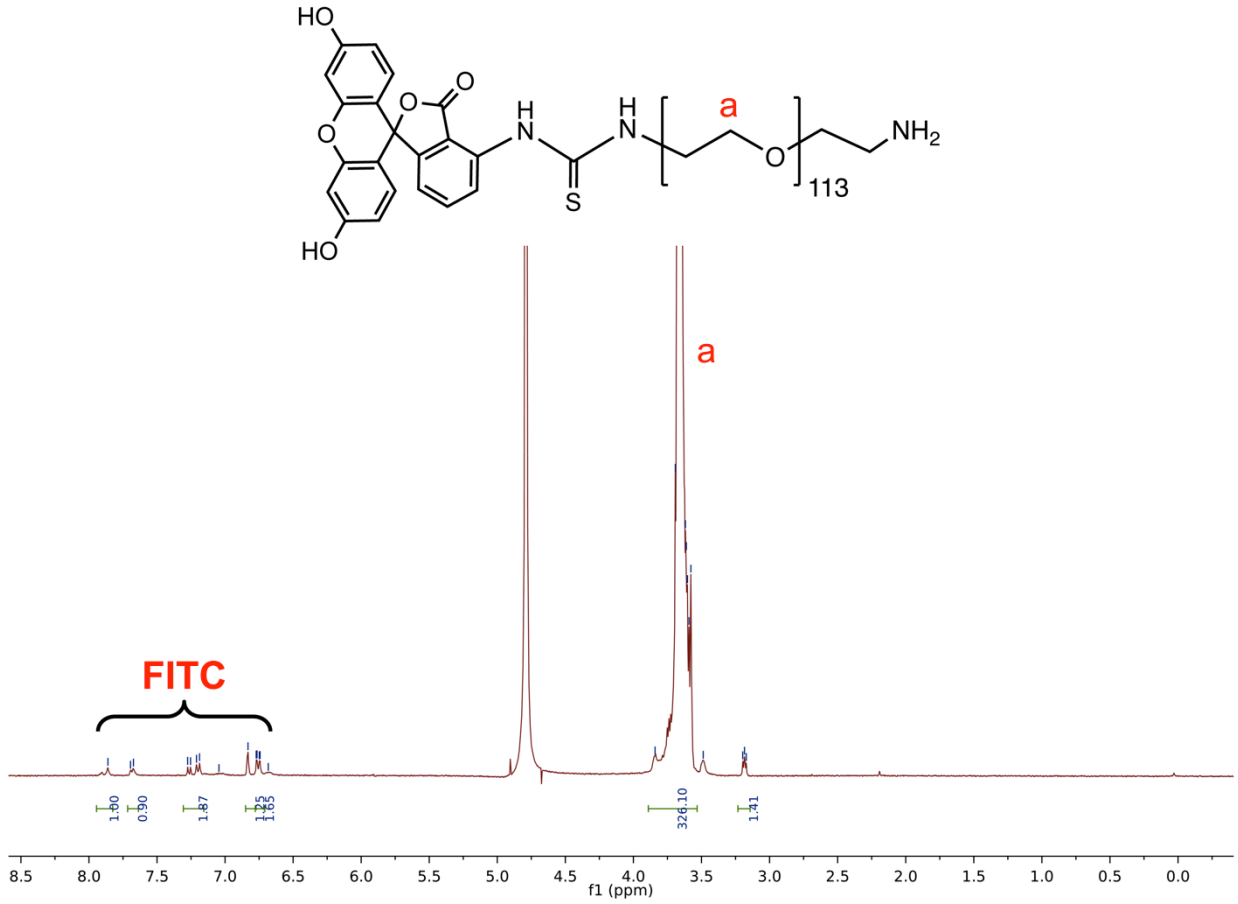

Figure S1. ^{1}H NMR spectrum of FITC-PEG5K-NH_2 in D_2O showing the characteristic peaks of FITC between 6.5 – 8.0 ppm.

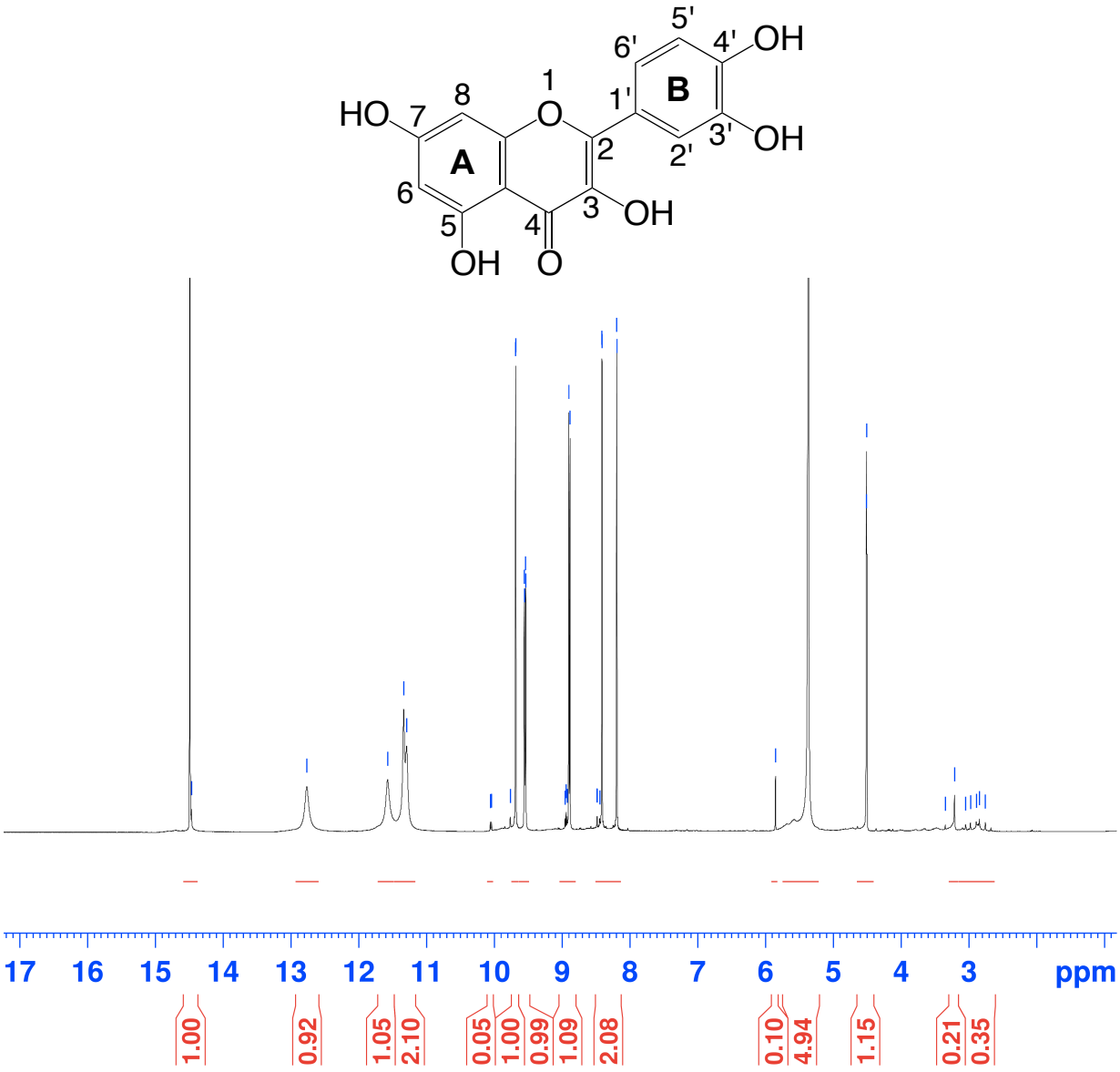

Figure S2. ^{1}H NMR spectrum of QCT (500MHz, DMSO-d_6) δ: 8.19 (1H, d, H-6), 8.41 (1H, d, H-8), 8.94 (1H, d, H-5'), 9.55 (1H, d, H-6'), 9.68 (1H, s, H-2'); 11.29 (1H, s, C7-OH), 11.33 (1H, s, C3'-OH), 11.57 (1H, s, C4'-OH), 12.77 (1H, s, C3-OH), 14.46 (1H, s, C5-OH) ppm.

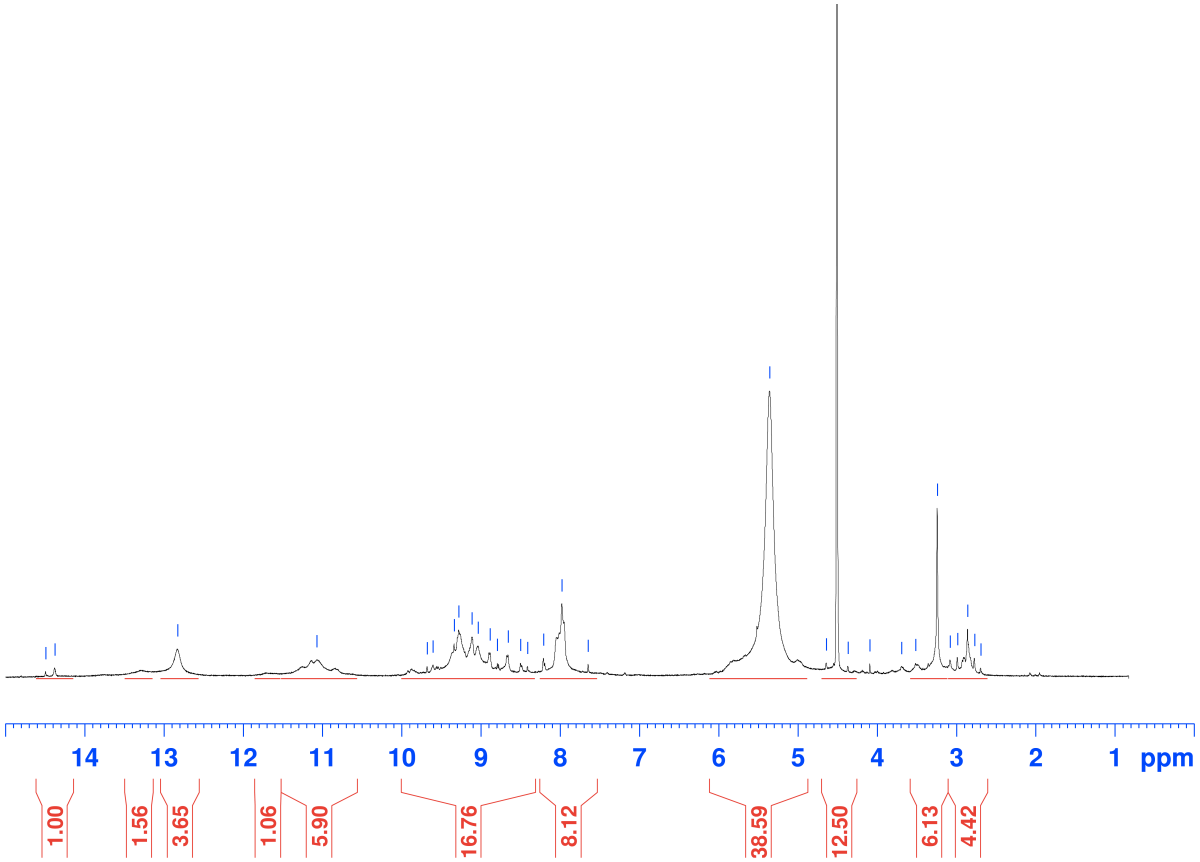

Figure S3. ^{1}H NMR spectrum of pQCT. The 5- and 2.6-fold increase in integration values of aromatic and -OH protons, respectively, strongly suggest that QCT oxidation has resulted in the formation of oligomers comprised of approximately 5 QCT monomers.

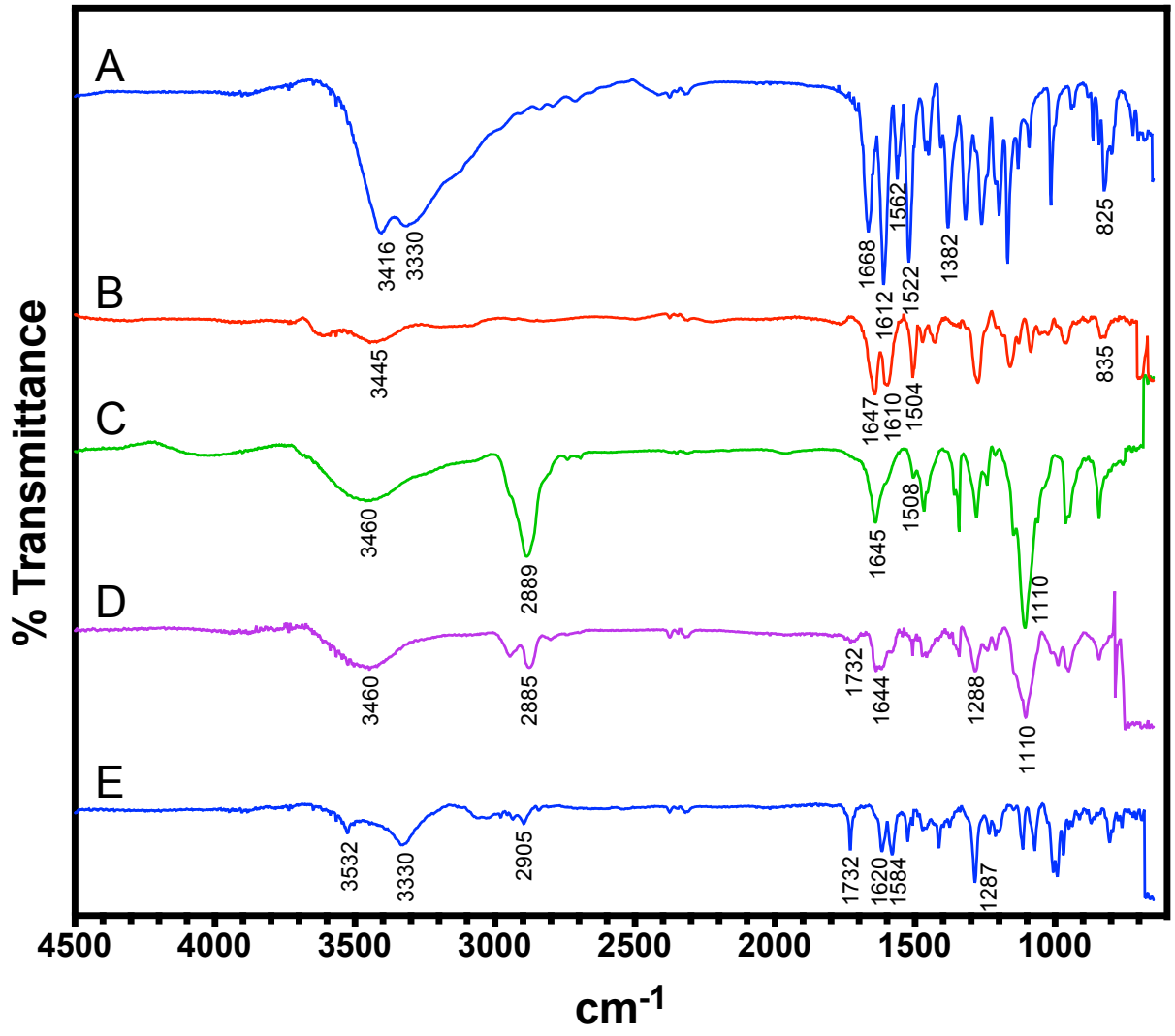

Figure S4. FT-IR spectra of (A) QCT, (B) pQCT, (C) pQCT@PEG, (D) pQCT@PEG@DOX, and (E) DOX.

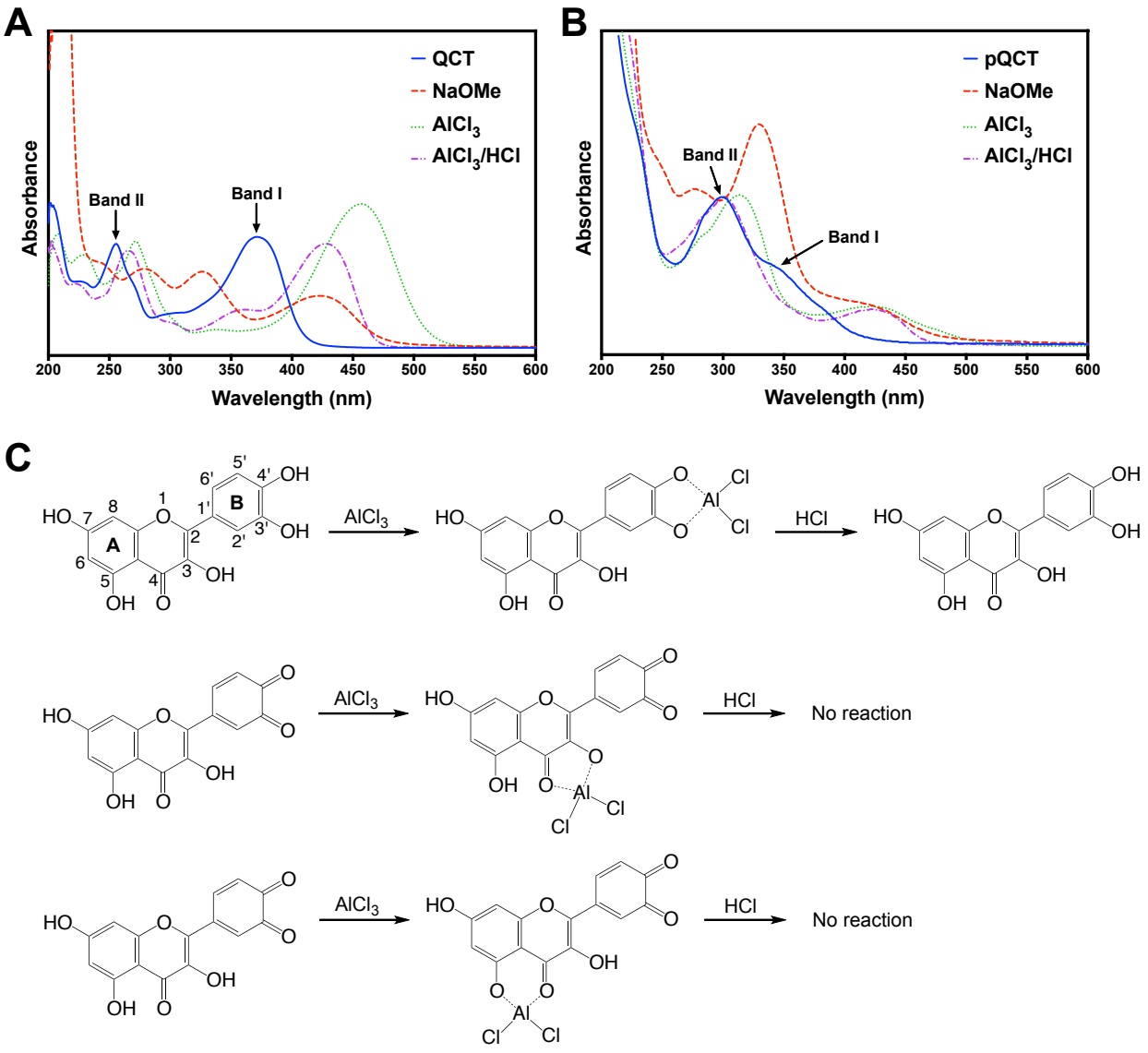

Figure S5. UV-Vis spectra of (A) QCT and (B) pQCT in methanol before and after the addition of NaOMe, $AlCl_3$, and $AlCl_3$/HCl. (C) Types of complexes that can form between $AlCl_3$ and QCT depending on the oxidative state of the *o*-dihydroxyl groups on ring B.

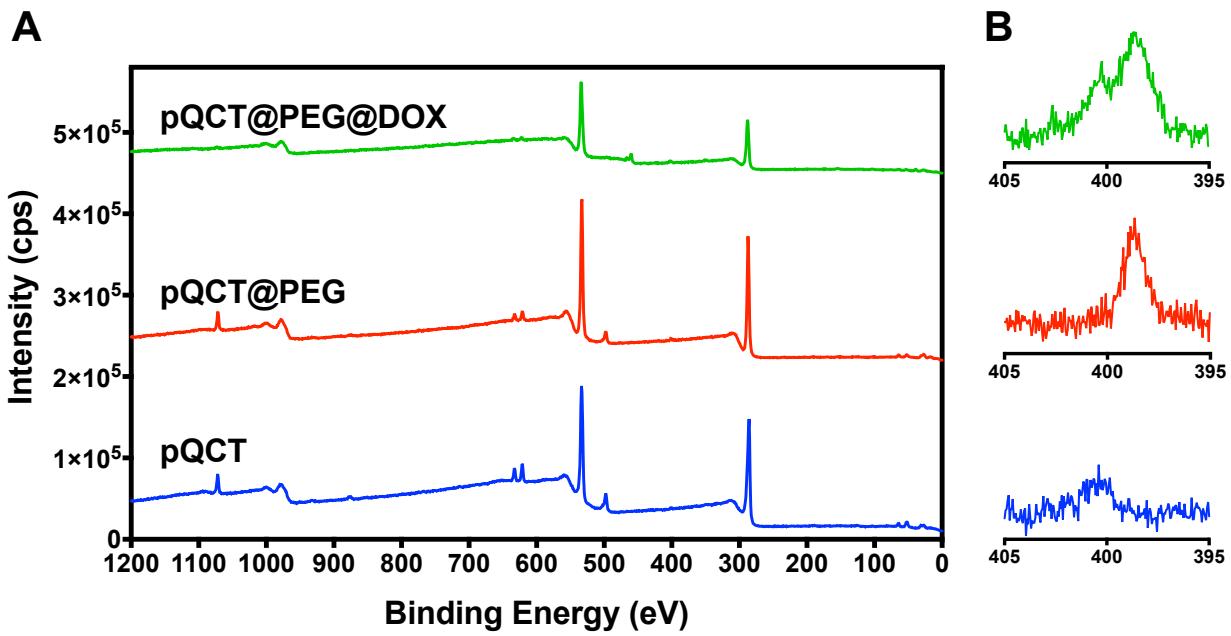

Figure S6. (A) Representative XPS Survey spectra of pQCT, pQCT@PEG, and pQCT@PEG@DOX NPs. (B) High resolution scans of the N 1s region for each sample showing a significant increase in N % upon PEGylation.

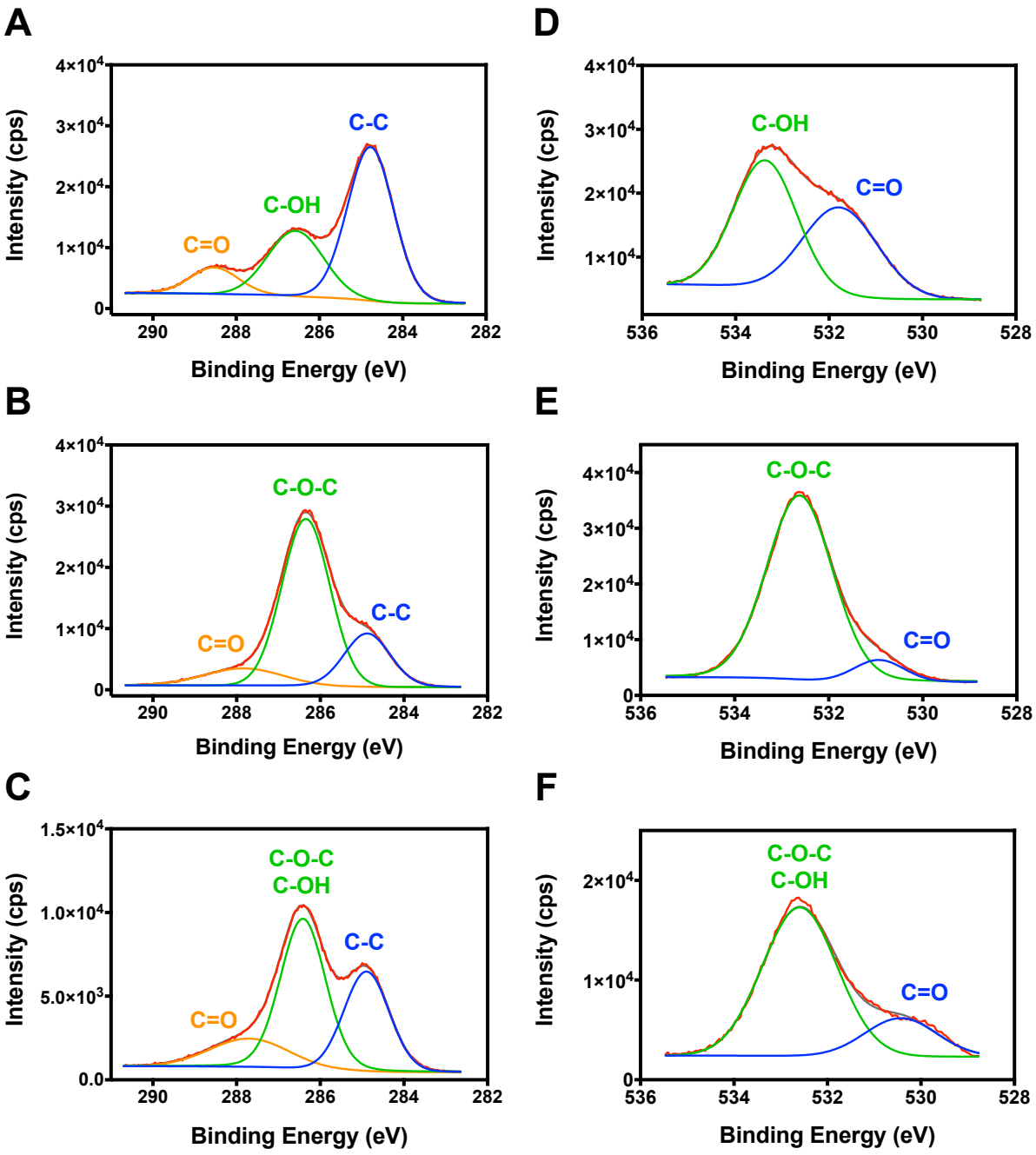

Figure S7. Deconvoluted high resolution scans of the C 1s (A-C) and O 1s (D-F) regions of pQCT (A and D), pQCT@PEG (B and E), and pQCT@PEG@DOX NPs (C and F), with peak assignments inferred from literature values. The increase in C-O-C components observed in B, C, E, and F compared to A and D is attributed to immobilization of mPEG-NH_2 on the surface of pQCT NPs.

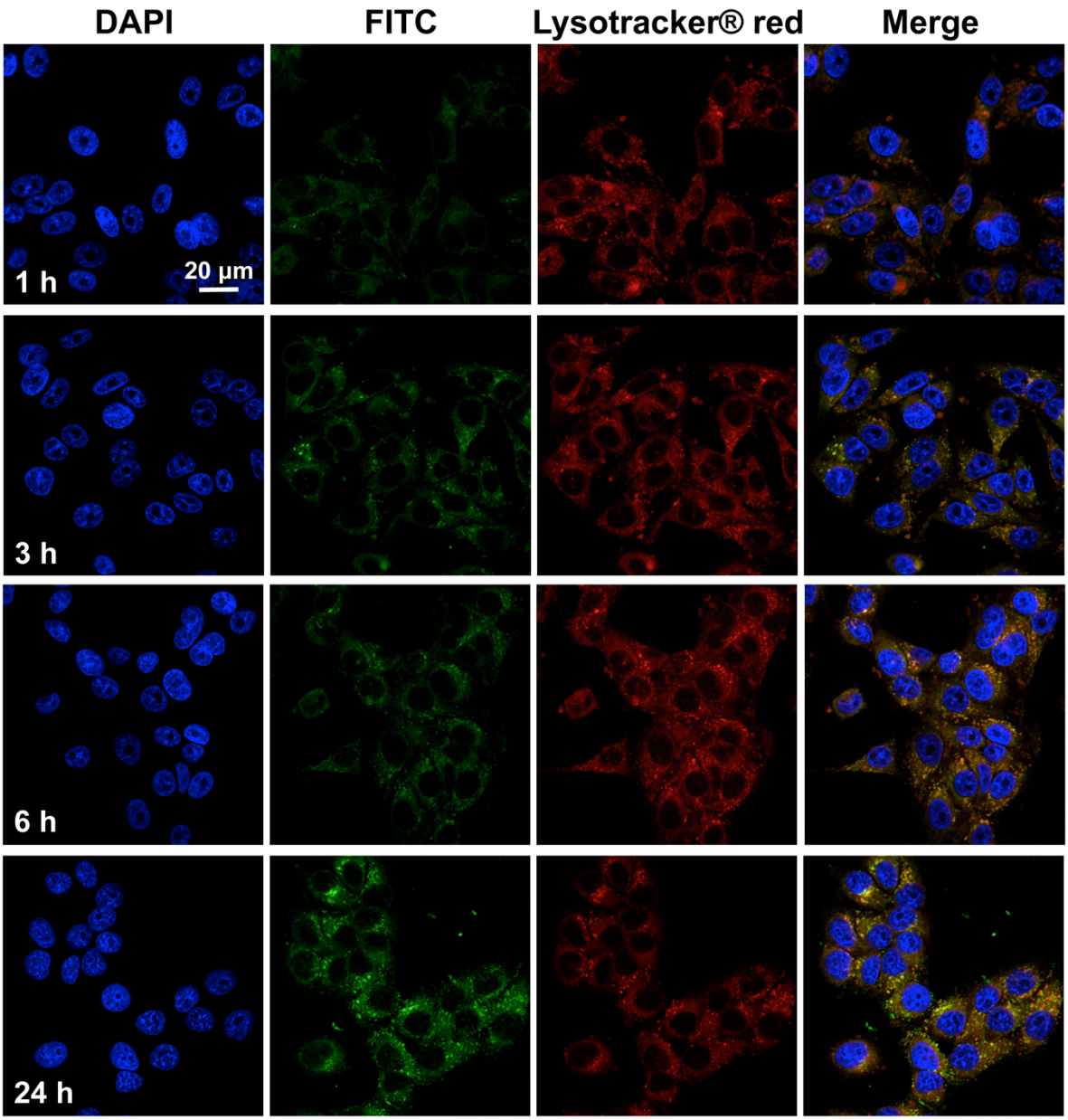

Figure S8. CLSM images of KB cells incubated with 10 μg/mL pQCT@FITC-PEG NPs up to 24 h showing time-dependent uptake of the NPs (blue channel: cell nuclei stained with DAPI; green channel: FITC-labeled NPs; red channel: LTR). Colocalization of green (FITC-labeled NPs) and red (LTR) fluorescence signals indicates the presence of the NPs in lysosomal compartments (Pearson's correlation coefficients of 0.62, 0.78, 0.72, and 0.71 for 1, 3, 6, and 24 h incubation, respectively).

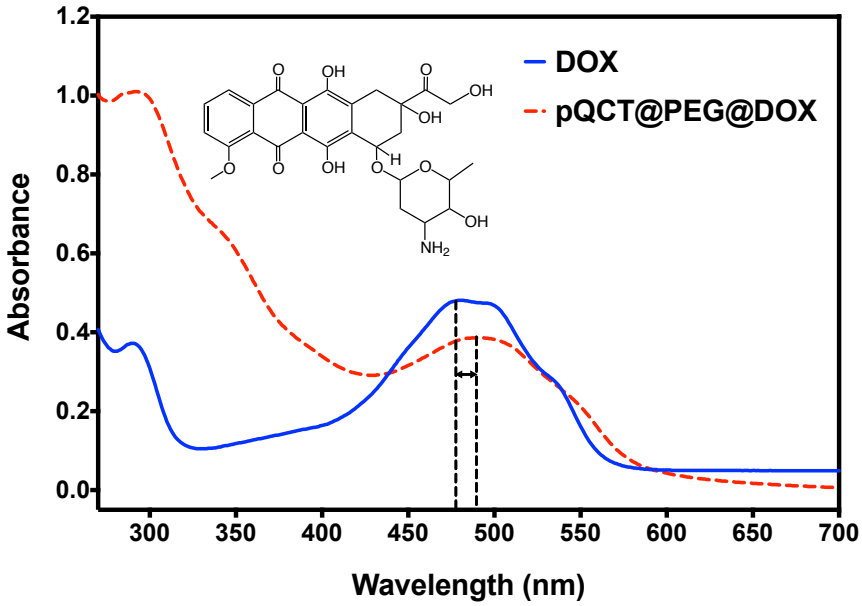

Figure S9. UV-Vis spectra of free DOX and pQCT@PEG@DOX NPs showing a shift in λ_{max} for DOX from 482 to 490 nm after loading onto the NPs.

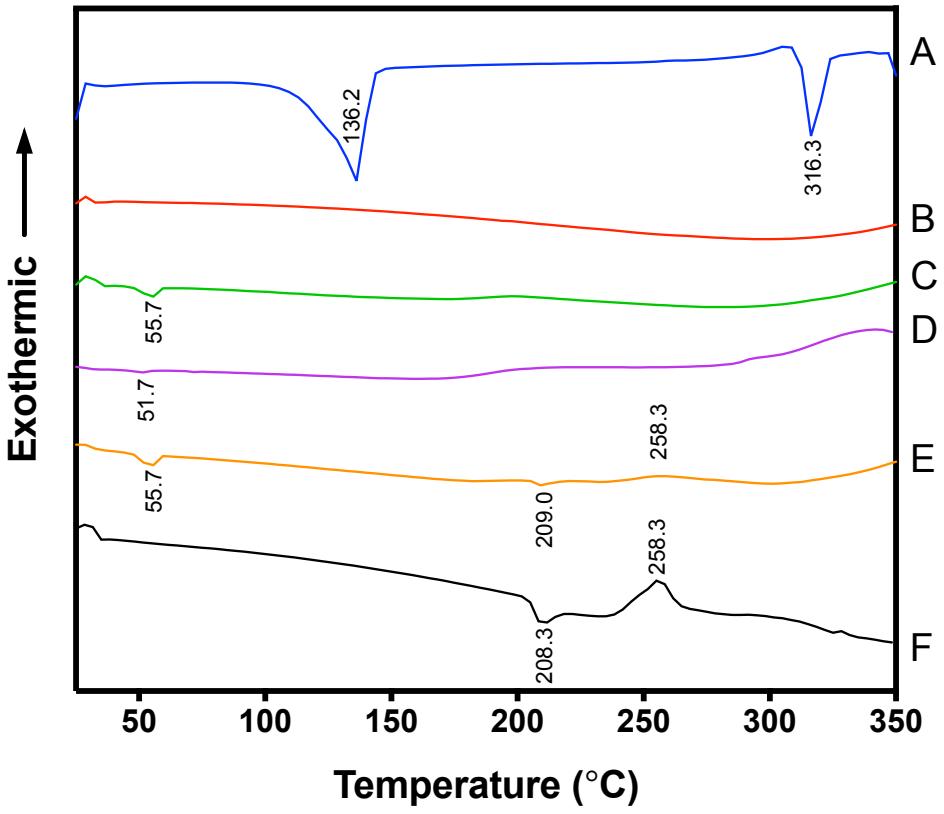

Figure S10. DSC thermograms of (A) QCT, (B) pQCT NPs, (C) pQCT@PEG NPs, (D) pQCT@PEG@DOX NPs, (E) pQCT@PEG/DOX physical mixture, and (F) DOX. QCT exhibited two sharp endothermic peaks at 136.2 and 316.3 °C. pQCT is an amorphous material with no characteristic thermal transitions. pQCT@PEG showed an endothermic peak at 55.7 °C. This peak was shifted to 51.7 °C and attenuated in pQCT@PEG@DOX NPs. DOX exhibited an endothermic melting peak at 208.3 °C, and an exothermic peak attributed to thermal degradation at 258.3 °C, which were both absent in the thermogram of DOX-loaded NPs. pQCT@PEG/DOX physical mixture showed thermal transitions similar to those observed in the DOX and pQCT@PEG individual curves.

A

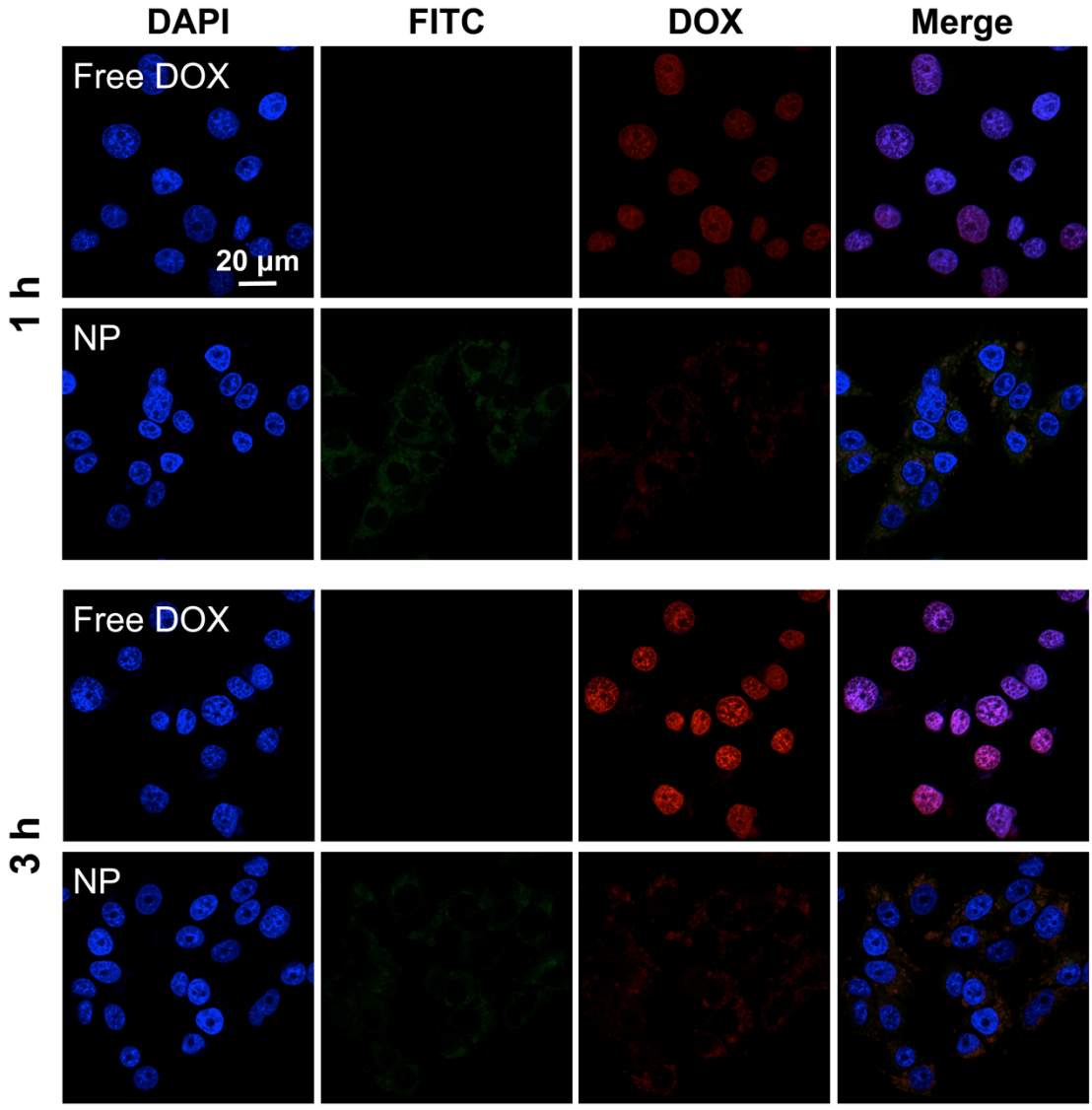

B

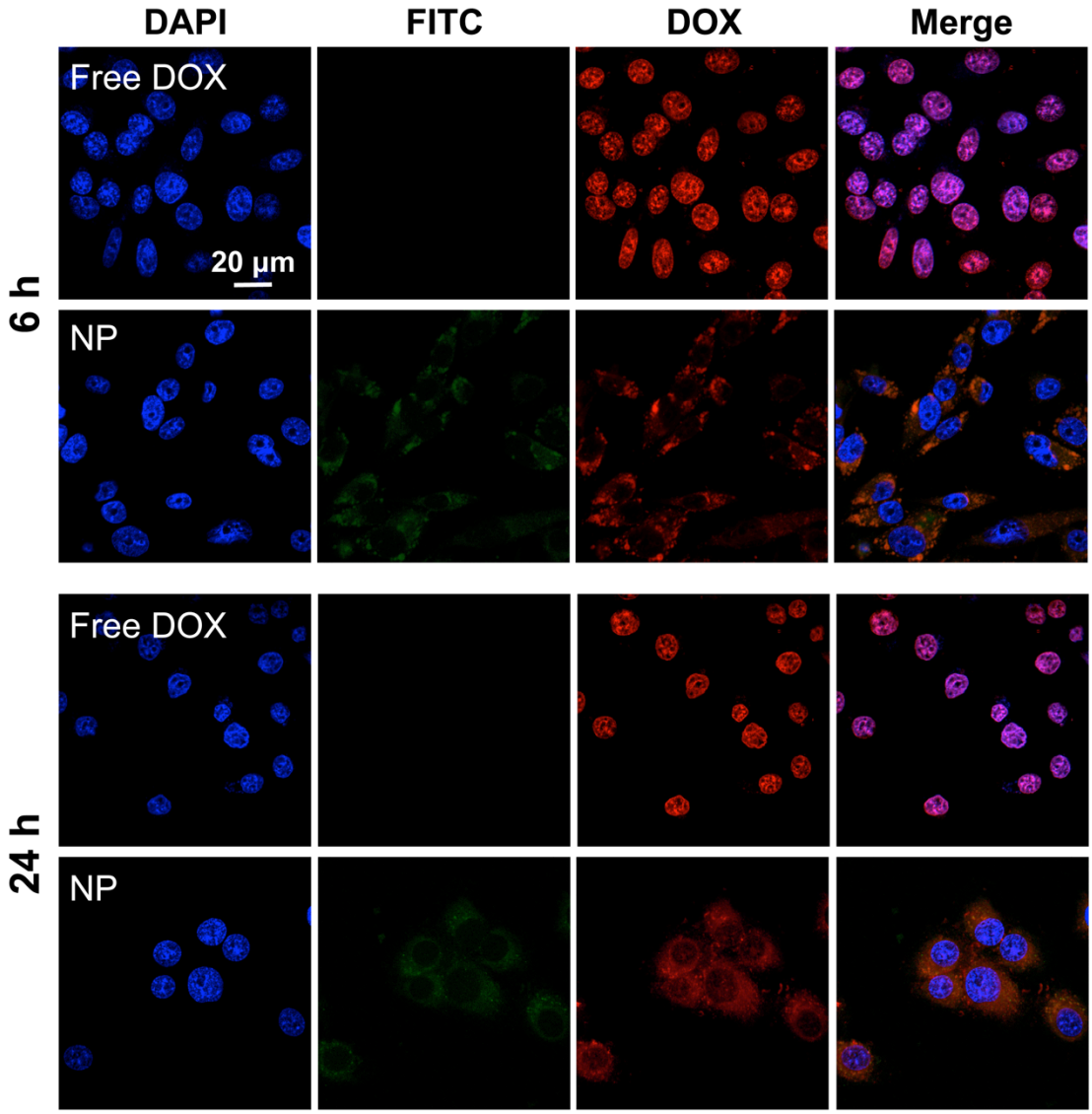

Figure S11. Cellular uptake of DOX from pQCT@FITC-PEG@DOX NPs in KB cells compared to free DOX (blue channel: cell nuclei stained with DAPI; green channel: FITC-labeled NPs; red channel: DOX). (A) CLSM images of KB cells after 1 and 3 h incubation with 5 μM free DOX and DOX-loaded NPs showing strong nuclear red fluorescence signals for free DOX but not the NPs due to insufficient drug release. (B) CLSM images of KB cells after 6 and 24 h incubation. Nuclear localization of DOX is observed at 24 h upon its release from pQCT@FITC-PEG@DOX NPs.

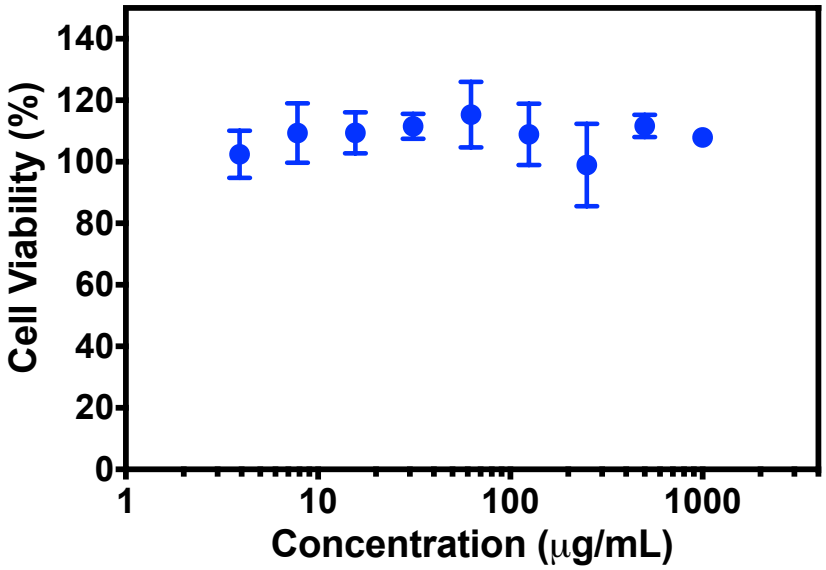

Figure S12. Viability of KB cells incubated with pQCT@PEG NPs up to 1 mg/mL in complete RPMI 1640 for 48 h. Results are plotted as mean ± SD of % cell viability obtained from three independent experiments.